Cyclic Behavior of Concentrically Braced Frames with Built-Up Braces Composed of Channel Sections

M. Nader Naderpour, Ali. A Aghakouchak*, and Amin Izadi

Department of Civil and Environmental Engineering, TarbiatModares University, 14115-111, Tehran, Iran

Abstract

Concentrically braced frames are earthquake resistant systems commonly used in buildings. Seismic behavior of this type of structures is affected by their configurations, brace properties, and brace to gusset plate connections. In this paper, the results of three experiments conducted to investigate the cyclic behavior of concentrically braced frames with braces built-up of double channels are reported. Significant damage was observed in beam to column connections. Large out of plane deformation of braces caused some cracks in the connector welds; however they did not result in fracture. Although large drift was applied to the frames, no brace fracture was observed. Furthermore, experiments showed that the majority of compressive strength in post-buckling state and a noticeable portion of tensile strength originated from frame action. By choosing connector spacing as the main parameter and using finite element models, a parametric study was performed to investigate the effect of this parameter on this type of frames with two different details of brace to gusset plate connections. It is observed that reducing the connector spacing increases the inelastic strain demand in braces and decreases it in gusset plates. However, gusset plates, which accommodate 2t linear clearance, are less dependent on connector spacing, compared to those accommodating 6t elliptical clearance. It seems that the limitations of slenderness ratio of individual section, stipulated in current seismic provisions, need further study.

Keywords: concentrically braced frames, built-up sections, gusset plate connections, connector spacing, experimental tests

1. Introduction

Concentrically braced frames, CBFs, are frequently used as a structural system to resist earthquake loading. High strength and stiffness as well as economic consideration have attracted engineers to this structural system. Seismic behavior of this type of frames is affected by their configurations; brace properties such as slenderness, section geometry, compactness, and details of brace to gusset plate connections. In the past, different studies have been undertaken on this kind of frames, which can be classified in three distinct categories. In the first category, the seismic behavior of CBFs have been investigated with respect to their configurations, e.g. frames with diagonal, X, and chevron braces or those with super-X. In the second category, details of connection of brace to gusset plates have been the main parameters of interest. The third category of research has concentrated on the effects of properties of the brace section such as geometry, slenderness ratio, and width to thickness ratio on the seismic behavior of CBFs. In the following paragraphs, some of the researches falling in the second and third categories are reviewed briefly.

With regard to the second research category, considerable attention has been given to rotation capability of brace end. Brace end rotation can be achieved by accommodating proper clearance length in the gusset plate. Figure 1 shows some variations of different clearance lengths in a gusset plate. As one of the first and major research in this area, (Astaneh-Asl1982, 1988 and Astaneh-Asl and Goel 1984) carried out some experimental full scale tests. In their study, 23 double angle braces, which were connected to gusset plates with different clearance lengths, were cyclically loaded. In these models, the linear clearance length of t, 2t and 4t were tested in which t is the gusset plate thickness.

They proposed a 2t linear clearance length in order to achieve a ductile behavior of CBFs. This recommendation has been later stipulated in seismic provisions and it still exists in Seismic Provisions for Structural Steel Buildings (AISC, 2010a). Although complying with the mentioned detail can bring more ductile behavior; it usually leads to big and thick gusset plates.

*Corresponding author
  Tel & Fax: +009882883322
  E-mail: a_agha@modares.ac.ir

(a) no clearance   (b) elliptical clearance   (c) linear clearance
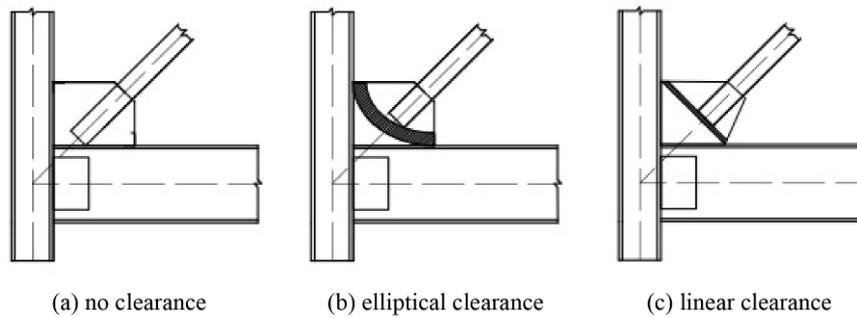
Figure 1. clearance length variation.

Some other researchers also examined the seismic behavior of concentrically braced frames focusing on connection details. Among these studies, extensive research has been done at University of Washington (Yoo *et al.*, 2008; Leman *et al.,* 2008; Lumpkin *et al.,* 2010; Roeder *et al.,* 2011). More than 30 frames have been tested experimentally. Based on their findings, the common procedures stipulated in (AISC, 2010a) have some shortcomings. To address these shortcomings, three suggestions were made. First, it was suggested that balanced design procedures (BDP) be used to design connections. BDP is based on balancing the damage mechanism of desirable yielding in order to avoid undesirable damage modes. It is obtained through a hierarchical design system of yielding and failure. Second, it was recommended that an elliptical 6t to 8t clearance length be used instead of a linear 2t one. Third, it was proposed that the welding of the interface of gusset to beams and columns be designed based on the plastic strength of gusset plate not that of the brace.

Some researchers have analyzed the test data on braces to explain the cyclic behavior of this structural member. (Tremblay, 2002) undertook a research by compiling the results of 76 tests in 9 studies done around the world. Buckling strength of braces, post-buckling behavior in different ductility levels, maximum tensile strength, out-of-plane deformation during buckling, and fracture life of braces were investigated. It was inferred that brace slenderness is the dominant parameter affecting the seismic behavior of braces. (Lee and Bruneau, 2005) performed another study similar to Tremblay by quantifying the energy dissipated in load cycles based on compiling data from 7 different studies. The dissipated energy in braces of different section and slenderness were investigated. The results demonstrated that compressive strength and energy dissipation capacity in compressive braces decrease dramatically for slenderness ratio over 80.

A number of studies have been done to investigate brace fracture in CBFs subjected to cyclic loading. Braces experience severe inelastic deformation due to buckling. The consecutive excursions of tensions and compressions in cyclic loadings lead to brace fracture, which occurs in 10-20 inelastic cycles. (Fell *et al.,* 2009) undertook 18

large-scale tests of steel bracing members of different section shapes to examine their inelastic buckling and fracture behavior. Based on their observations, they proposed a micromechanics-based fracture model to explain the test results. It was concluded that width to thickness ratio was the most important parameters affecting the seismic behavior of brace members. Since micro-mechanical approaches are costly and time-consuming, some other researchers such as (Hsiao *et al.*, 2013), (Takeuchi and Matsui, 2014), (Lai & Mahin, 2014), (Uriz, 2015) adopted macro-based approaches to predict brace fractures. The main idea in their research is to calculate cumulative strain to predict the fracture of the braces. Based on their studies, they have proposed some models for brace fracture prediction.

Previous studies have shown that frame action can largely contribute to CBF resistance and stiffness and also affect the whole behavior of the CBF (Roeder *et al.,* 2011). (Stoaks and Fahnestock, 2010) studied the flexural behavior of frames, which are normally used in CBFs. Some subassemblies of column, beam and gusset plate have been considered. They investigated the reserve capacity of the frames with different beam-column connections with gusset plate, which employ double angle and end plate details, to examine the effect of connection details on stiffness and strength of those frames. The study concluded with comparing the strength, stiffness and ductility of different connection details.

(Lee & Bruneau, 2008a; 2008b) conducted 12 tests on built-up laced brace members. The brace sections were built up by two or more single sections tied by laces leading to braces with different slenderness and width to thickness ratios. The buckling modes, buckling and post buckling strengths were reported as well as the results of analytical studies. They compared the ductility of different built-up sections and concluded that sections with larger global slenderness (kl/r) and smaller local slenderness (b/t) dissipated larger energy than others. Another study by (Jiang *et al.,* 2012) developed a fiber based model to model built-up braces composed of double angles in OpenSESS. They validated the results of their proposed model against experimental results and claimed that the model was capable to model this type of

built-up braces.

Based on above review, although many studies have been done on the behavior of CBFs, only a few ones have considered CBFs with built-up sections. Out of these, very few have studied the braces built-up of channels. Nevertheless; AISC Seismic Provision of Steel Buildings (AISC, 2010a) has stated some criteria for built-up sections to ensure the ductile behavior of these structures. As a step to bridge the gap on this area, this study tries to investigate the seismic behavior of this type of frames experimentally and numerically.

In this paper, the results of 3 half-scale tests are reported. Two tests were designed to examine the cyclic behavior of CBFs whose braces are built up of double channels. The other one was a bare frame tested to determine the contribution of frame in the whole behavior of CBFs. The frames were then simulated numerically and the results were compared to experimental ones. Finally, a parametric study was conducted to understand the effects of details of connections of individual channels to each other and to the gusset plates on the overall behavior of CBFs.

2. Experimental Program

Experimental program consisted of 3 frames. Based on the limitations of our laboratory, half-scale specimens needed to be tested. Figure 2(a) shows the experimental setup schematically. As it is illustrated in this Figure, two compressing jacks were used in order to apply the cyclic loads. Two load cells were used to measure the applied force. A beam was used to prevent the out-of-plane deflection of the frame by constraining the top of the columns. Figure 2(b) shows the frame bay and height dimensions. Each frame was connected to the strong floor using pin connections at the bottom of the columns. In order to measure the displacements, several linear variable differential transformers (LVDTs) were located on the frame so that the top and bottom frame displacements as well as out-of-plane displacement of the brace and gusset plate could be monitored. The specimens were whitewashed to help observe the yielded regions visually. Still photographs along with videos were taken to record the events throughout the test.

In designing the frame elements, an intermediately slender brace was selected. The brace sections were built-up by two channels connected face to face with connectors. Figure 3 shows the built-up details. As it can be seen in Figure 3(a), there is a gap between two channel sections equal to the gusset plate thickness. At each side of the brace, there are some connectors in the form of batten plates, which stitch the two channels together (Fig. 3(b)). The connector plates are welded to the channel flanges at both sides and at a specific distance using fillet welds (Fig. 3(c)). The connector distances are given in Table1. Each individual channel is connected to the gusset plate

(a)

(b)
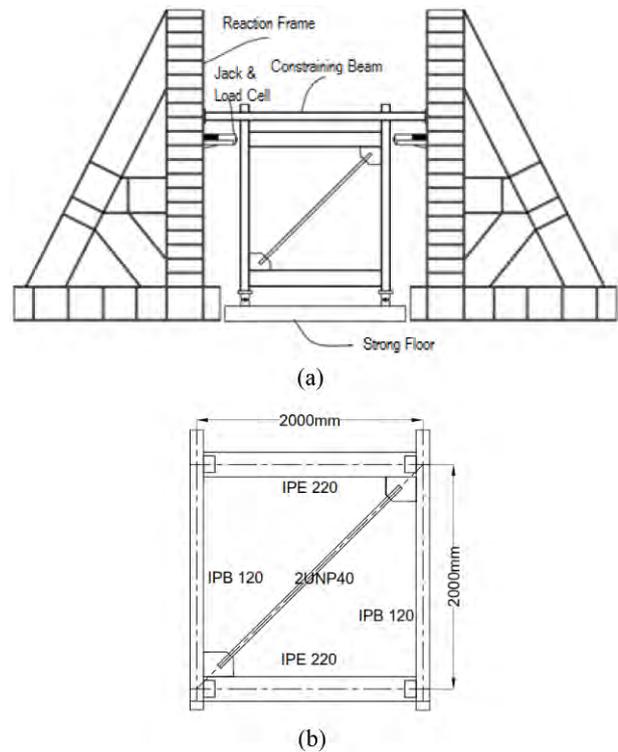
Figure 2. Schematic presentation of (a) test set-up (b) frame sample

by fillet welding the two flanges of that channel to the gusset plate (Fig. 3(d)). The connection of this type of brace to the gusset plate is quite similar to connection of hollow squared section (HSS) brace to the gusset plate. However in this type of connections there is no need to make a slot in the brace and consequently there is no need to reinforce the brace for net section failure. Based on the capacity of the brace section, the columns and beams of the frame were designed so that they could resist the forces developed in these elements. The gusset plates were designed on the basis of the ultimate strength of brace. Gusset plate dimensions were designed to assure no premature failure in brace to gusset plate connections. In Table 1, the element details for each specimen are presented. The sections used in this study, are all hot-rolled known as standard European sections. 2UPN40 denotes the built-up sections composed of two UPN40x 20 channels. Table 2 provides more information on the sections used in this study. Table 3 shows the weld sizes used in different connections of three specimens tested in this study.

ATC-24 loading protocol (ATC 1992) related to far field ground motions was selected. Figure 4 shows the loading protocol applied to the specimens. The quantities of each cycle and its amplitude as well as the maximum drift in each cycle are presented. The loading is quite symmetrical so in each cycle, the maximum amplitude in tension and compression is the same.
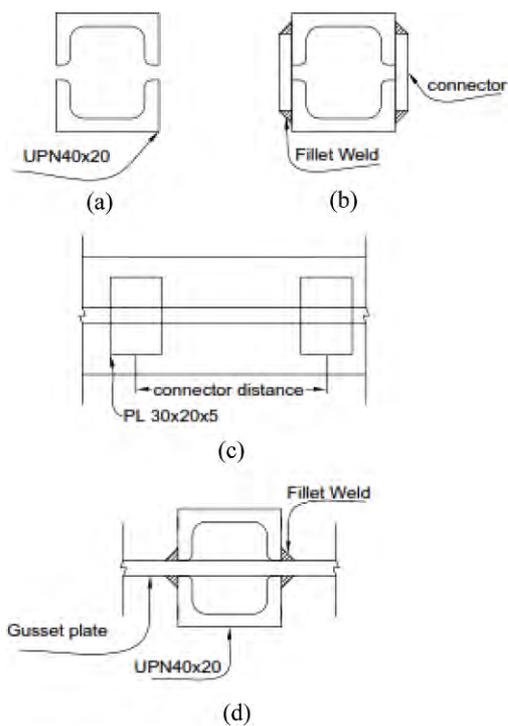
Figure 3. built-up brace (a) general section (b) section where there are connectors (c) longitudinal view of brace d) brace to gusset plate connection.

As it can be seen in Table 1, the columns and beams of all specimens are the same. Specimens 1 & 2 have similar braces but the connection details differ. Specimen 3 is identical to test 2 except that it is not braced.
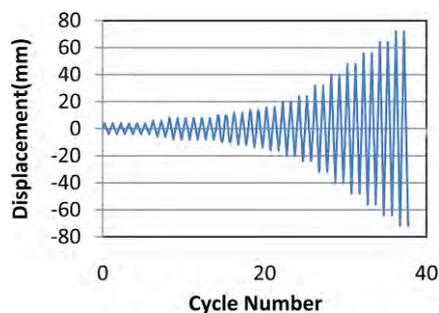
Cycle Quantity	Maximum Amplitude (mm)	Maximum Drift Ratio (%)
6	4	0.2
2	6	0.3
6	8	0.4
2	10	0.5
2	12	0.6
2	14	0.7
2	16	0.8
2	20	1
2	24	1.2
2	32	1.6
2	40	2
2	48	2.4
2	56	2.8
2	64	3.2
2	72	3.6

Figure. 4. Cyclic loading protocol.

Table 1. Details of frame specimens

Specimen	Column	Beam	Gusset plate	Brace	Clear length of brace (mm)	Connector Distance (mm)
1	IPB120	IPE220	Rectangular, 6 mm thick, Elliptical 6t clearance	2UPN40	2080	695
2	IPB120	IPE220	Rectangular, 6 mm thick, no clearance	2UPN40	2090	695
3	IPB120	IPE220	Rectangular, 6 mm thick	-	-	-

Table 2. Section properties

Section	Area (mm^2)	Depth (mm)	Flange width (mm)	Web thickness (mm)	Flange thickness (mm)
IPB120	3400	114	120	6.5	11
IPE220	3340	220	110	5.9	9.2
UPN40x20	370	40	20	5	5.5
2UPN40	740	40	46	5	5.5

Table 3. fillet weld size of different connections (mm)

Specimen	Gusset plate to Beam	Gusset plate to Column	Brace to Gusset Plate	Shear tab to Beam	Shear tab to Column	Connector to Brace	Angles to Beam/Column
1	6	6	5	6	6	4	5
2	6	6	5	6	6	4	-
3	6	6	-	6	6		-

2.1. Specimen No. 1

In this specimen the brace is built up by connecting two UPN40x20 channels face to face. The brace is 2080 mm long with a slenderness ratio $(KL/r)_o$ of 140, which is categorized as an intermediately slender brace. The rectangular gusset plate accommodates an elliptical 6t clearance proposed by (Roeder *et al.*, 2011). The beam is connected to column using a shear tab and two angles. The shear tab connected the beam web to the column flange using fillet weld on all sides. Two 100 mm long angles of 30×30×5 were used at the top and bottom of the beam to connect the beam flanges to the column flange using fillet welds. This detail used to be common in some buildings so it was adopted in this specimen. Figure 5(a) shows the gusset to beam-column connection and also beam to column connection. Two connectors at each side of the brace (totally four connectors) connect the two channels dividing the brace length into three equal segments. The slenderness ratio of individual section between two connectors (a/r_i) is 105. Considering the total slenderness ratio and the latter, the modified slenderness ratio $(Kl/r)_m$ of the brace, as per (AISC 2010b) is calculated following Eq. (1).

$$\left(\frac{Kl}{r}\right)_m = \sqrt{\left(\frac{Kl}{r}\right)_o^2 + \left(\frac{a}{r_i}\right)^2} = 175 \qquad (1)$$

The gusset plate was designed based on the welding length required to resist the ultimate tensile force of the brace as well as the length needed to connect gusset plates to beam and column. Each brace flange is connected to the gusset plate using fillet welds. The fillet weld sizes are presented in Table 3.

2.2. Specimen No. 2

This specimen is generally identical to Specimen No. 1; however there were two differences. First, the gusset plate detail was different. In this model, no clearance was provided in gusset plate details. This is due to the fact that in the past, quite a number of structures used to be designed and constructed without accommodating end clearance, which deserve attention for the purpose of retrofit strategies. Second, the beam to column connection was different so that the beam was connected to the column using a shear tab which was fillet welded on all sides. There was a gap of 10 mm between the beam flange and column flange in order to enable beam rotation. Figure 5(b) illustrates the two connections in this frame. The gusset plate dimensions in this specimen were designed to resist the entire force developed in braces and the welding length required to transfer loads to beam and column.

2.3. Specimen No. 3

Past experience has shown that whilst in the braced frames, the beam to column connection may not be a moment resisting one, nevertheless due to the existence of the gusset plates, a relative fixity is created. Thus the frame contributes to resisting the lateral force, which has beneficial as well as detrimental subsequences. In this regard, a model was designed to determine this contribution. To serve this purpose, while fabricating Specimen No. 2, another identical frame was also fabricated with similar gusset plates but without any brace element. Figure 5(c) shows the connection detail of this specimen. As it is shown the connection details of this specimen are exactly the same as Specimen No. 2.
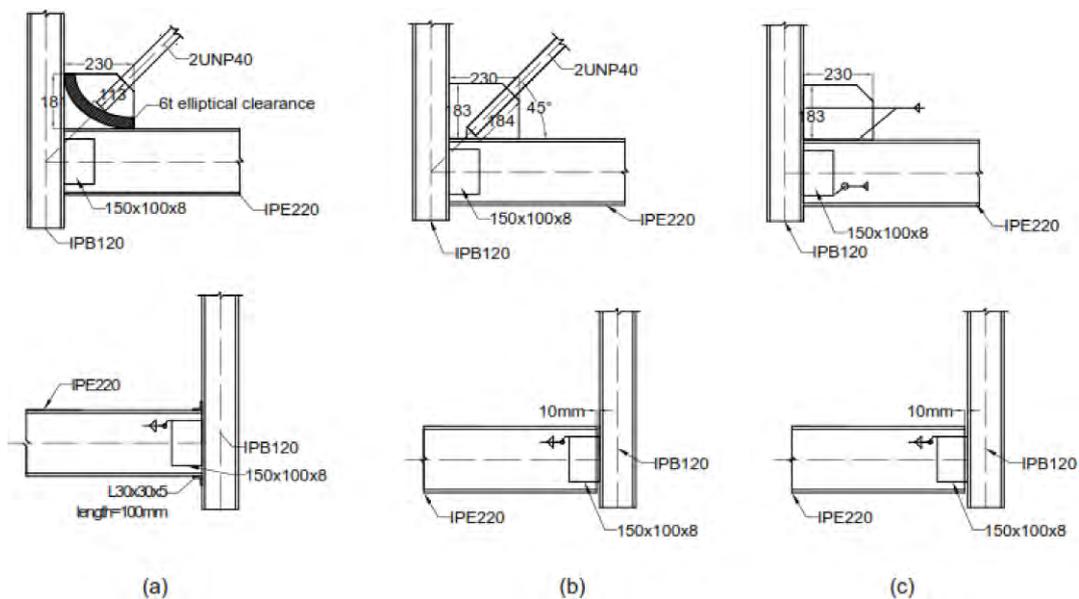
Figure 5. Connection details of (a) Specimen No. 1, (b) Specimen No. 2 (c) Specimen No. 3 (all dimensions are in millimeter)

Table 4. Material properties

Shape	Measured property	
	F_y(MPa)	F_u(MPa)
Brace	340	510
Beam	300	440
Column	305	450
Gusset plate	280	415

2.4. Material properties

Coupon specimens were prepared from the materials used for brace, beam, column, gusset plate and uniaxial tensile tests were carried out. The material properties are given in Table 4.

3. Test results, Observations and Discussion

3.1. Test 1

By applying cyclic loads on Specimen No. 1, the global buckling of the brace occurred at 0.4% drift ratio (DR). This indicated first inelastic event at early cycles. The brace buckled at the lower half of the brace whereas the brace was completely symmetrical. By increasing the load amplitude, whitewash flaking was observed at the bottom of the column, where the beam was connected to the column at 0.5% DR. As the load increased, the out-of-plane deformation of brace grew resulting in high demands on the gusset plate corner. Figure 6 shows this deformation. The high demands initiated cracking in the interface of gusset plate to column. A crack of an approximate length of 2 mm was observed at gusset plate corner at 2% DR. On the other hand, crack initiation was observed in the connections of the beam to column at the bottom particularly on the side that there was no gusset plate. As the out-of- plane deformation of the brace increased, the two sections of channels forming the brace came to contact with each other making significant noise throughout the test. As the test continued, small cracks in the connector welds appeared at 2.4% DR. However, they did not fracture till the end of test. As the frame drift increased, more tearing appeared especially in the column to beam connections. When the amplitude reached 3% drift, the frame was pushed monotonically up to 5% drift. Contrary to all expectations, the brace did not fracture but significant tearing was observed in the connections of beam to column, which was responsible for part of the drift observed in the frame. Figure 7 shows the experimental hysteretic curve.

3.2. Test 2

The sequence of events in this model was largely similar to that of Test 1. The brace buckled at 0.38% drift ratio. Similar to test 1, the buckling point was not at the middle of the brace. Then, flaking of whitewash occurred at the base of the column at 0.6% DR. Later, crack

Figure 6. Large out-of-plane deformation of brace in Test 1.
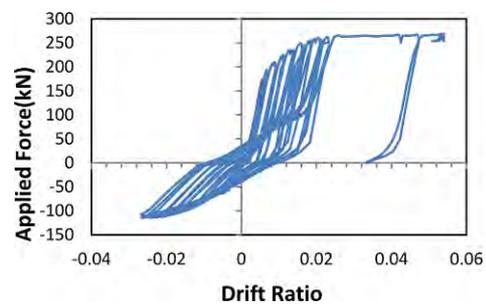
Figure 7. Experimental hysteresis curve of Test 1.

initiated in the connection of bottom beam to column at 0.9% DR. As more load cycles were applied, the crack propagated gradually. Crack started at 2.3% DR at the top corner of bottom gusset plate. The test ended at 2.7% DR due to complete separation of beam and column. Although the brace did not fracture, the brace underwent fairly large out-of-plane deformations causing the two sections of channels to deform significantly. Figure 8 shows frame deformation at the last step of the test.

The deformation history of specimens No. 1 and 2 were similar. The experimental hysteretic curve is presented in Fig. 9.

3.3. Test 3

This test is in fact a companion to Test 2. Figure 10 shows the setup of this test. Since there was no brace in this structure, almost all the inelastic events occurred in the connections of beams to columns. Whitewash flaked at the bottom of the column at 0.6% DR. Moreover, the first visible damage was observed in the bottom of the frame where the beam was connected to the column without gusset plate. The crack initiated in the connection at 1.2% DR and gradually propagated till the connection tore and the beam was completely separated at 3% DR. The other connection at the bottom also cracked. However, due to the existence of gusset plate, it experienced less damage compared to the other one. Figure 11 shows the connection status at the last stages of the test. In Fig. 12

Figure 8. Large post buckling deformations in Test 2
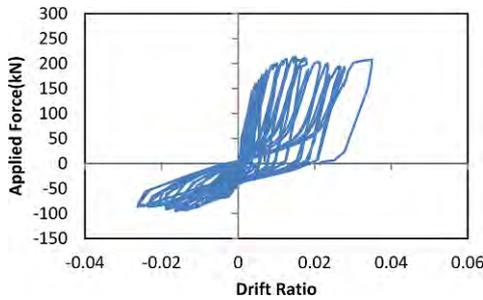
Figure 9. hysteresis curves of Test 2.

Figure 10. Setup of test 3.

Figure 11. crack in connection of beam to column in test 3.
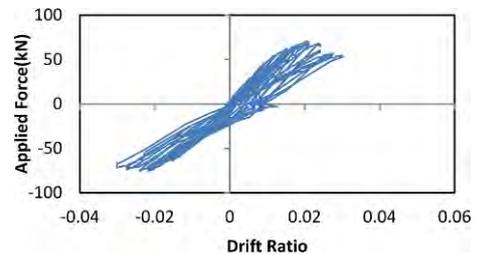
Figure 12. Experimental hysteresis curves of Test 3.

Figure 13. Deformations of braces (a) Test 1 (b) Test 2.

the hysteretic curve obtained from this experiment is shown. The values of frame strength in tension and compression are almost equal.

3.4. Discussion on experimental observations

In the preceding sections, the observations of the tests were presented. Two main differences existed in Test 1 and Test 2 setup. The first difference lay in the brace to gusset-plate connection and the other in the beam to column connection detail. Due to longer welding length

in brace to gusset plate connections in specimen No. 2, more brace end rigidity could be observed in specimen No. 2 in comparison to specimen No. 1. Figure 13 shows deformed specimens at the same state. The global deformation shapes were the same; however more fixity was seen in Test 2.

By comparing the hysteretic curves of Test 1 and 2, it was observed that in the post-buckling zone of the hysteretic curve of Test 1, there was a bigger pickup in compressive and tensile strength which is attributed to greater frame action of Test 1 compared to Test 2. The maximum tensile strength of Test 1 is approximately 250 kN while it is 200 kN for Test 2. On the other hand, the maximum compressive strength is about 108 and 83 kN for Test 1 and 2, respectively. This difference stemmed from the angles attached the beam to the column. The

angles caused more fixity in the beam to column connections and therefore greater frame action. This type of connection also resisted more cycles than the simple connection which used a shear tab to connect the beam web to the column flange. Test 1 stopped at 5% DR due to jack stroke shortage while Test2 stopped at 3% DR owing to complete separation of beam to column. This phenomenon can be also seen in the hysteretic curve of Test 2 where both tensile and compressive strength of the frame experienced strength deterioration as a consequence of damage occurred in the specimen.

Drawing a comparison between hysteretic curves of Test 2 and 3 revealed that the majority of frame strength in compression (about 88%) originated from frame action, i.e. the ultimate strength of Test 2 was 84 kN while it was 74 kN for Test 3. Nonetheless, the tensile strength of Test 3 is about 33% of that of Test 2.

4. Numerical Simulation of Experimental Models

The cyclic behavior of experimental models was also investigated numerically. For this purpose, a finite element model, FEM, was created for each specimen using ABAQUS (Simulia, 2011) platform. Each model was constructed considering all the elements existing in experimental model and then it was subjected to the specific cyclic displacement history presented in Fig. 4. Four-node shell elements with reduced integration and five points of integration through the thickness were considered. Several models with different mesh sizes were constructed to determine the mesh size required to ensure accuracy of the FE results while optimizing the run time. Based on the modeling, an approximate mesh size of 10 by 10 mm was used for brace and connection zones where high plastic deformations were expected. A coarser mesh of about 50 by 50 mm was used in column and beam regions where limited plastic deformations were anticipated. Connections such as brace to gusset plate, gusset plate to beam and column, connector to channels and shear tab to column were simulated by merging the two surfaces in the FEM software. Shear tab to beam connections were modeled by tying the edges of shear tabs to beam webs. The main limitation of this simulation is that it is not able to capture weld crack initiation and propagation. By performing a buckling analysis, an initial imperfection was applied to the model, which was proportional to the first buckling mode and its amplitude was equal to 1/1000 of the brace length in the middle of the brace. Figure 14 shows the FE model of the Specimen No. 2 from different views. A rigid triangular plate attached to the base plate was used to simulate the pin connection existing in experiment. The top and bottom of the flange columns were restrained to prevent out-of-plane translations in order to model boundary conditions. Material properties were considered based on the results
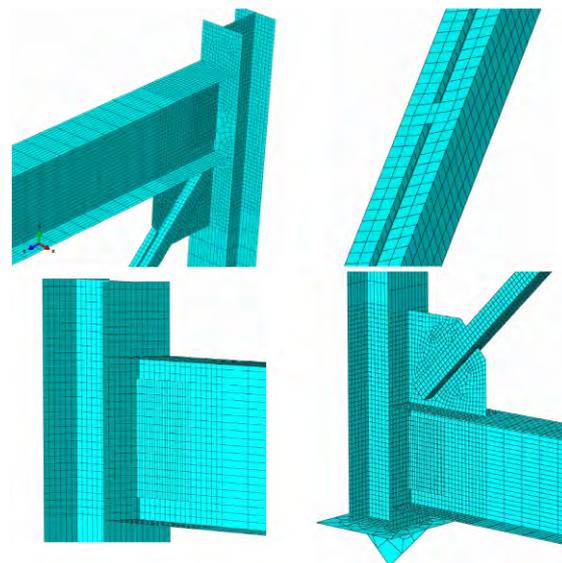
Figure 14. Different views of specimen No. 2 FE model.
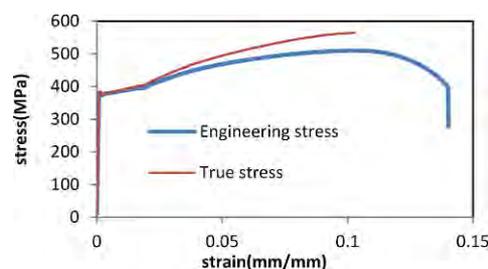
Figure 15. Stress-strain curve of brace elements.
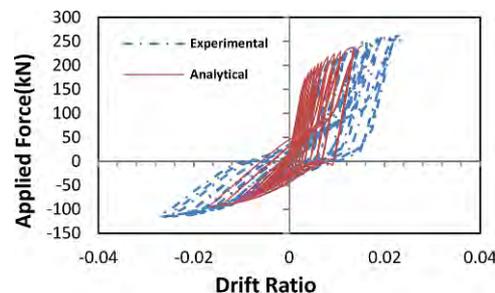
Figure 16. Numerical vs. experimental results of Test 1.

obtained from tension coupon tests, as shown in Table 4. The engineering stress strain curves obtained by tensile tests were converted to true stress-strain curves and then used in the software. Figure 15 shows the brace stress-strain curve as a sample. A kinematic hardening rule was selected. Experimental curves of the three specimens were presented in preceding sections. In Figs. 16 through 18 they are re-presented comparing them with numerical results.

As it can be seen in the Figs. 16 and 17, the general behavior of frames obtained from analyses and experiments are in agreement. In test 1, the numerical analysis for last few cycles did not converge; therefore the results are
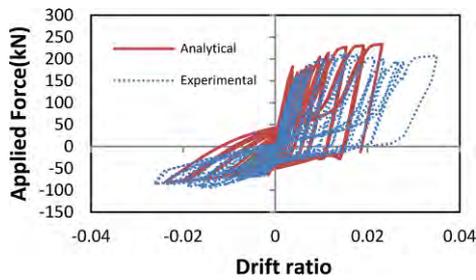
Figure 17. Numerical vs. experimental results of Test 2.
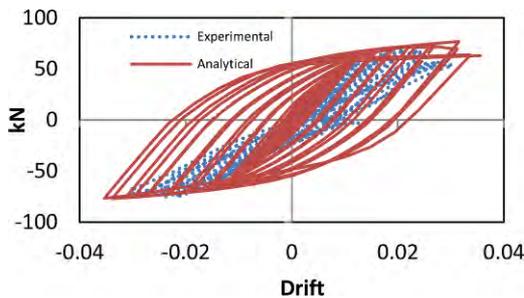
Figure 18. Numerical vs. experimental results of Test 3.

presented only for the cycles that the results have converged. In test 2, the strength of the frame is lower than the numerical model, which is because of local damage in frames primarily due to fractures in welded connections. Both frame 1 and 2 experienced a strength pick-up after brace buckling in compression that can be attributed to frame action. During unloading in both of Tests 1 and 2, a difference in numerical and experimental results is observed. The disagreement associated with unloading is more evident in Fig. 18.

It must be noted that in FE models, cracking was not modeled and material properties did not model any damage either. As a result, stresses and strains continue to increase in the vicinity of connections regardless of the phenomena such as weld crack and tearing that actually happened during experiments. However, these events would not affect the total hysteretic curves of braced frames like specimen 1 and 2 unless the frame experiences considerable damage. The case appears to be different for specimen 3. This specimen does not have any brace so all the stiffness and strength come from the connections. Therefore, every single crack can affect the stiffness and strength of this frame. It can be observed that the stiffness decreases significantly as the test proceeds. The strength starts to decline in drift ratios over 2%.Nonetheless; the FE model predicts the initial stiffness and ultimate strength fairly well.

The numerical models could simulate local behavior to a great extent. The models predicted the unsymmetrical buckling of the braces like what was observed in experiments. Figure 19a shows the deformation modes observed in the test vs. analytical prediction. Figure 19b shows Mises stress in the brace near its connection to
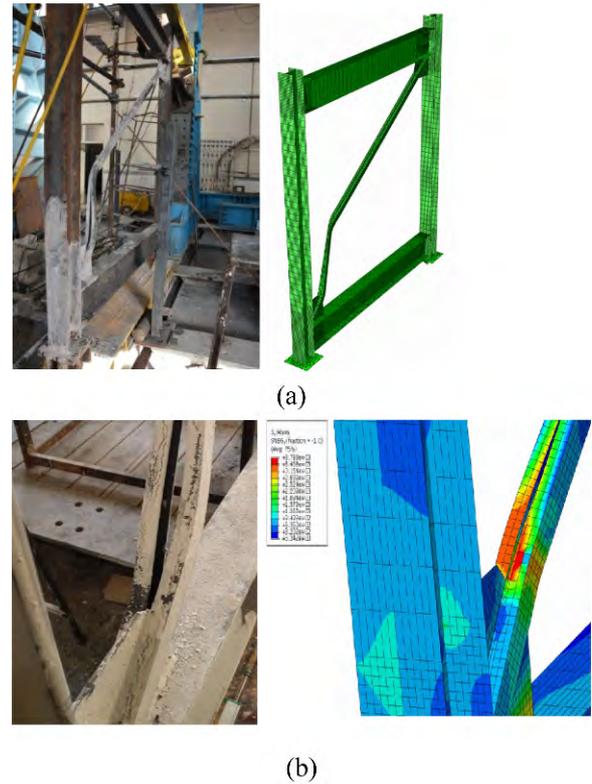
Figure 19. Experimental vs. analytical results (a) brace buckling shape of Specimen No. 2 (b) Mises stress in brace near gusset plate and whitewash flaking in Specimen No. 1.

gusset plate. High stress can be observed in the flange and the web there. In experiment, whitewash flaking was observed which shows high stress in that area too.

5. Parametric Study

To further investigate the behavior of CBFs with built-up braces, a parametric study has been done. This study focuses on connectors tying the two channels along the brace length. Design provisions (AISC, 2010a) for structural buildings prescribe some regulations for SCBFs with built-up braces. However, no specific regulations are stated for built-up braces of OCBFs, which means that general regulations for built-up sections included in (AISC, 2010b), suffice. The seismic provisions states that: "The spacing of connectors shall be such that the slenderness ratio, a/r_i, of individual elements between the connectors should not exceed 0.4 times the governing slenderness ratio of the built-up member". The following parametric study intends to examine the effect of connector spacing as a parameter on the whole seismic behavior of CBFs. In this regard, by changing the distance between the connectors to slenderness ratio of brace, different models were generated. Two different gusset plate details including 6t elliptical clearance length and 2t linear clearance length were considered. An

Table 5. Characteristics of numerical models

Name	Brace Length (mm)	$\dfrac{KL}{r}$	$K\dfrac{a}{r_i}$	$\left(\dfrac{KL}{r}\right)_m$	$\dfrac{a/r_i}{(KL/r)}$
Bu40-E6t-C2	2326	135	107	172	0.79
Bu40-E6t-C3	2326	135	80	157	0.59
Bu40-E6t-C4	2326	135	64	150	0.47
Bu40-E6t-C5	2326	135	53	145	0.39
Bu40-E6t-C6	2326	135	46	143	0.34
Bu40-L2t-C2	2300	134	105	170	0.78
Bu40-L2t-C3	2300	134	79	155	0.59
Bu40-L2t-C4	2300	134	63	148	0.47
Bu40-L2t-C5	2300	134	53	144	0.40
Bu40-L2t-C6	2300	134	45	141	0.34

intermediately slender ratio of about 135 was considered. All the models are half-scale models similar to those tested experimentally. The same approach taken for numerical modeling of experimental tests, i.e. loading protocol, material definition, element selection, mesh size, etc. was adopted.

5.1. Model characteristics

In Table 5, the characteristics of numerical models are presented. In the nomenclature used to refer to each model, three parameters are involved. The first term refers to brace section, which stands for Built-up of 2UPN40 and is shown as Bu40. The second term refers to gusset plate detail which stands for Elliptical 6t or Linear 2t clearance length shown as E6t and L2t respectively. The third term refers to the numbers of connectors used for each individual section to tie them together. Other information including slenderness ratio, modified slenderness ratio and the ratio of individual section between two connectors to the whole slenderness ratio is also provided in Table 5. The beams and columns of all the frames are identical to experimental models. Figure 20 shows the connection details of the numerical models containing the beam-column with gusset plate connection as well as beam to column connection.

As it can be seen in Fig. 20 two types of connection for beam-column with gusset plate connections were considered. However, the beam to column connection for all the models was the same and is illustrated in Fig. 20(c).

5.2. Damage measure

Numerical modeling of the frames is carried out using the FE method. Hence, the simulation is only valid until there is only plasticity in the model. However, as it was observed in the experimental studies, large damage in the form of cracking or tearing may occur in the frames, when they are subjected to larger drift ratios. By comparing the numerical models of tested specimens and experimental observations, equivalent plastic strain (ε_e^p) can be used as
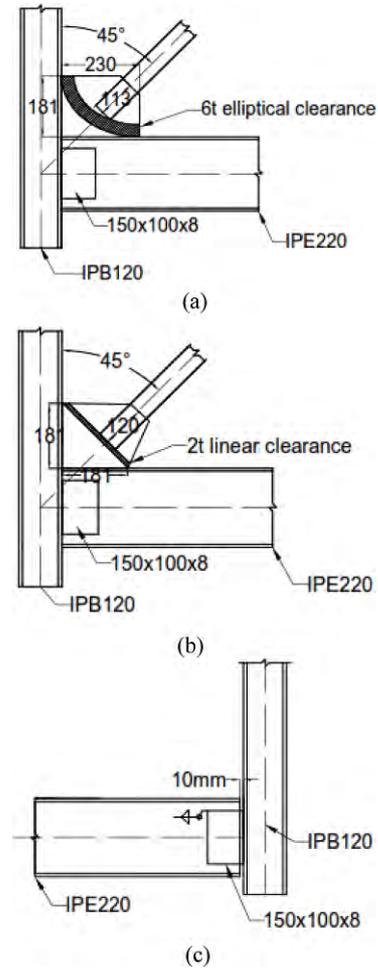
Figure 20. Connection details of parametric models (a) Bu40-E6t type (b) Bu40-L2t type (c) beam to column connection.

a proper index to consider initiation of cracking. Precise study of fracture needs more sophisticated tools, however for the purpose of comparing the potential of cracking, which is the intent of this paper; equivalent plastic strain can provide a good insight. Due to high dependence of this index on mesh sizing, equal mesh sizes were adopted in critical locations of all models.

6. Numerical Results

In this section, the numerical results obtained from analyses are presented. Then the effects of connector spacing in two different gusset plate details are investigated. In Fig. 21, the hysteretic curves of Bu40-E6t-C2 and Bu40-E6t-C6 models are shown. They are selected since these two models have most difference compared to other models. However, their hysteretic behavior does not seem to differ significantly. The other models have fairly similar hysteretic curves, but they are not presented in Fig. 21. As it can be inferred from the diagrams, in the range of studied models, the connector spacing does not have

significant effect on the strength and stiffness of hysteretic curves. It is obvious that tensile capacity of the frame strongly depends on the net area of brace, which is constant in all models. Nonetheless, it is expected that when the brace is subjected to compression, the difference in connectors spacing, which affects the compression strength of the brace, results in different behavior of frame. However, as the majority of compression strength of the frame in post-buckling state of the brace, is from frame action, the effect of connector spacing is over-shadowed. The same pattern can be observed in the hysteretic curves of Bu40-L2t (Fig. 22). It implies that for the range of studied models, connector spacing has no significant effect on hysteretic curves in frames with gusset plate complying 2t linear clearance.

Considering numerical results and experimental observations, three locations are considered to be critical with regard to cracking. One is in the connection zone, where the beam is connected to the column and ruptures were observed throughout the tests; the other one is in the brace and the last one is in the corner of gusset plates. Since the damage in connection is highly dependent on its detail and the detail is the same in all models, it is not discussed here. To compare the performance of frames, plastic equivalent strain (PEEQ) diagrams in two locations are investigated. Figure 23 shows PEEQ values of Bu40-E6t type. From Bu40-E6t-C3 through Bu40-E6t-C6, in which the distance between connectors is decreasing, the value of PEEQ is increasing. In other words, for the range of $0.34 \leq \dfrac{a/r_i}{(KL/r)} \leq 0.59$,

as this ratio decreases the values of PEEQ increase. Fig 24 shows the same pattern for Bu40-L2t type. From these two figures it may be said that reducing the space between two connectors, for the range mentioned above, results in a higher curvature of brace between the two connectors in buckled state and consequently in higher PEEQ. Figure 25 shows the state of two frames with different connector space at the same load cycles. Among numerical models, there are two models with $\dfrac{a/r_i}{(KL/r)}$

greater than 0.75, which do not comply with (AISC 2010b) specification for built-up members. PEEQ values of Bu40-E6t-C2 are higher than that of Bu40-E6t-C3, which do not follow the pattern described above indicating that cracking may initiate in the former model earlier. However for Bu40-L2t models, although, spacing of Bu40-L2t-C2 connectors exceeds the allowed one, it follows the mentioned pattern.

Decreasing the distance between brace connectors causes a different pattern in gusset plates. As the space between two connectors decreases, the value of PEEQs decreases as well. In other words, when the demand on brace increases, the gusset plates experience a lower demand. Figures 26 and 27 show the PEEQ diagrams for
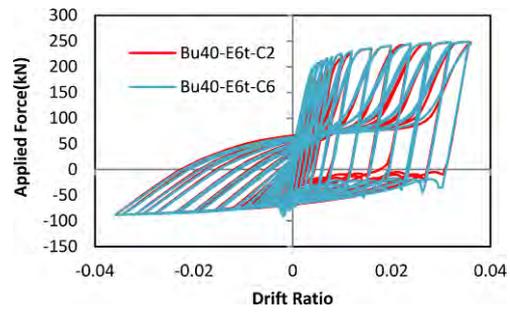
Figure 21. Hysteretic curves of Bu40-E6t type.
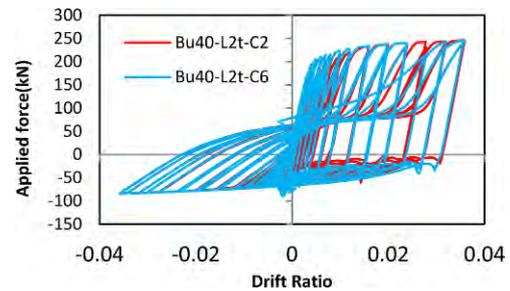
Figure 22. Hysteretic curves of Bu40-L2t type.
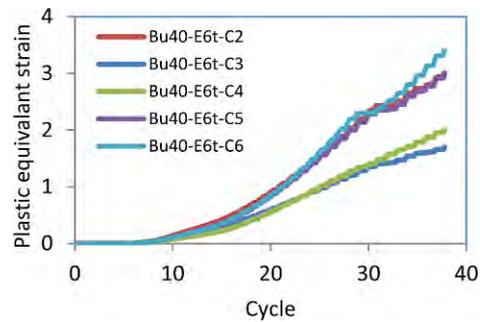
Figure 23. Plastic equivalent strain in critical point of the brace in Bu40-E6t type.
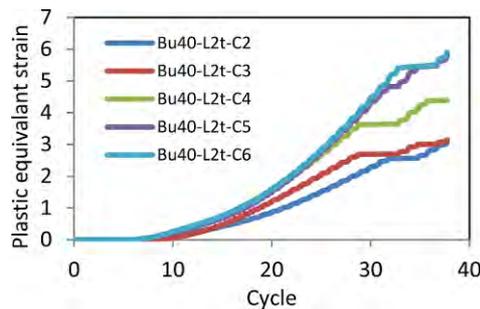
Figure 24. Plastic equivalent strain in critical point of the brace in Bu40-L2t type.

Bu40-E6t and Bu40-L2t types respectively. Although a similar pattern has been observed in both types, PEEQ is less dependent on connector spacing in Bu40-L2t type compared to Bu40-E6t type. This observation can be explained by the fact that when linear 2t clearance is provided, the majority of inelastic events occur in brace.
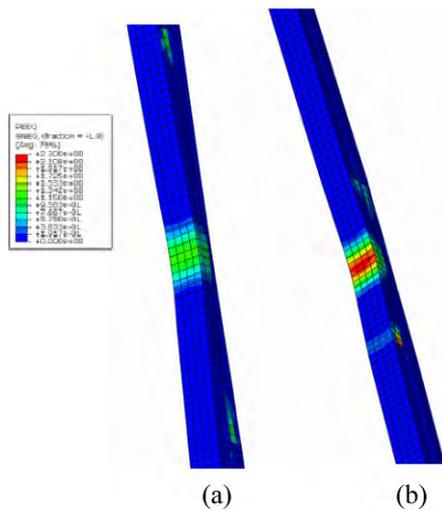
Figure 25. PEEQ contour of (a) Bu40-L2t-C3 (b) Bu40-L2t-C6
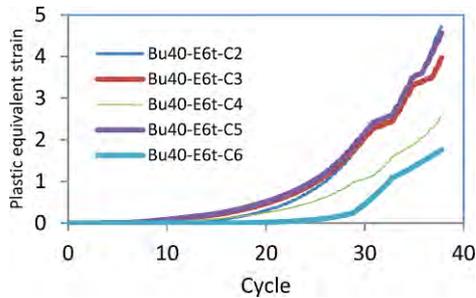
Figure 26. Plastic equivalent strain in critical point of the gusset in Bu40-E6t type.
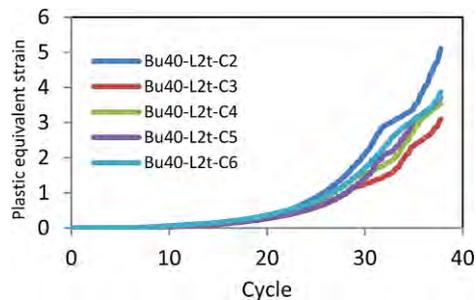
Figure 27. Plastic equivalent strain in critical point of the gusset in Bu40-L2t type.

Figure 28 displays the PEEQ contours of Bu40-L2t-C4 with Bu40-E6t-C4 at the same increment.

7. Summary and Conclusions

In this paper, the cyclic behavior of concentrically braced frames with braces built-up of channel sections was investigated. Based on the results of experimental and numerical studies, the following conclusions are drawn:

(1) In this type of frames, damage may be expected in beam to column connections, gusset plate corners and in
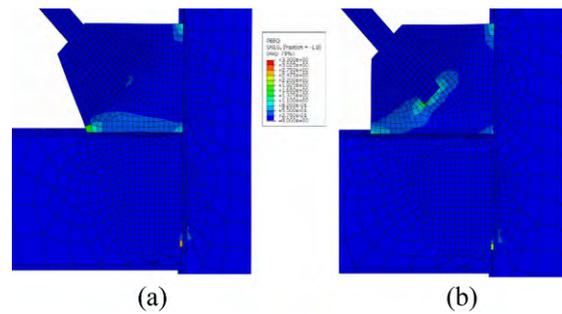
Figure 28. PEEQ contour of (a) Bu40-L2t-C4 (b) Bu40-E6t-C4.

connector welding along the braces during cyclic loading. However, in the reported experiments, although significant damage was observed in connection, minor cracks in gusset plate corners and connector welding occurred.

(2) Although quite a number of cycles with high drifts in last cycles (about 3% in each direction) were applied to the frames and the braces were fairly slender, no fracture was observed in braces. One reason can be the low width to thickness ratios of flange and web of the brace sections, which were about 3.7 and 8 respectively.

(3) Frame action plays an important role in compression strength of the whole frame especially in post-buckling state of brace. According to the test results, 88% of the compression strength belonged to the frame action in this state. On the other hand, this action is highly dependent on details of connection of beam to column. This phenomenon can dominate the damage sequence of frame. Although, AISC commentary (AISC 2010a) proposes some details to reduce frame action, for existing structures, further studies seem to be necessary.

(4) For the range of studied models, connector spacing does not affect the hysteretic curves of frames considerably. Frames with different connector spacing but the same brace and gusset-brace details have almost the same hysteretic curves from the stiffness and strength point of view.

(5) Reducing connector spacing of CBFs, which falls in the range of $0.34 \le \dfrac{a/r_i}{(KL/r)} \le 0.59$, leads to higher PEEQ in braces. Nonetheless, it decreases the PEEQ in gusset plate corner.

(6) Gusset plate PEEQs of frames providing 2t linear clearance and falling in the range mentioned above, are less dependent on connector spacing. In other words, by reducing the connector spacing in frames accommodating 2t linear clearance, the cyclic behavior does not necessarily improve neither from strength nor crack initiation points of view.

(7) It seems that the regulation stipulated in AISC Seismic Provisions (AISC 2010a) limiting the slenderness ratio of individual section (a/ri) for SCBFs is open to question and needs further study.

References

AISC (2010a).”Seismic Provisions for Structural Steel Buildings”. ANSI/AISC 341-10 American Institute of Steel constructions, Chicago, Illinois.

AISC (2010b). “Specification for Structural Steel Buildings”. ANSI/AISC 360-10, American Institute of Steel constructions, Chicago, Illinois

Astaneh-Asl, A. (1982). “Cyclic Behavior of Double Angle Bracing Members with End Gusset Plates”.

Astaneh-Asl, A. (1998). “Seismic Design and Behavior of Gusset Plates”. Structural Steel and Educational Council {Steel Tips}, 209.

Astaneh-Asl, A., &Goel, S. C. (1984). “Cyclic in-Plane Buckling of Double Angle Bracing”. *Journal of Structural Engineering*, 110(9), 2036-2055.

ATC (Applied Technology Council). (1992). “Guidelines for Cyclic Seismic Testing of Components of Steel Structures for Buildings.”

Fell, B. V., Kanvinde, A. M., Deierlein, G. G., & Myers, A. T. (2009). “Experimental Investigation of Inelastic Cyclic Buckling and Fracture of Steel Braces”. *Journal of Structural Engineering*, 135(1), 19-32.

Hsiao, P. C., Lehman, D. E., & Roeder, C. W. (2013). “A model to simulate special concentrically braced frames beyond brace fracture”. *Earthquake engineering & structural dynamics*, 42(2), 183-200.

Jiang, Y., Tremblay, R., & Tirca, L. (2012). “Seismic Assessment of Deficient Steel Braced Frames with Built-Up Back-to-Back Double Angle Brace Sections Using Opensees Modelling”. *Proceedings of the 15WCEE*.

Lai, J. W., &Mahin, S. A. (2014). “Steel Concentrically Braced Frames Using Tubular Structural Sections as Bracing Members: Design, Full-Scale Testing and Numerical” Simulation. *International Journal of Steel Structures*, 14(1), 43-58.

Lee K and Bruneau M (2008a).“Seismic Vulnerability Evaluation of Axially Loaded Steel Built-up Laced Members II: Evaluations,” *Earthquake Engineering and Engineering Vibration,* 7(2), pp. 113-124

Lee K and Bruneau M (2008b), “Seismic Vulnerability Evaluation of Axially Loaded Steel Built-up Laced Members II: Evaluations,” *Earthquake Engineering and Engineering Vibration*, 7(2), pp. 125-136

Lee, K., & Bruneau, M. (2005). “Energy Dissipation of Compression Members in Concentrically Braced Frames: Review of Experimental Data”. *Journal of structural engineering*, 131(4), 552-559..

Lee, Kangmin, and Michel Bruneau. (2008)”Seismic vulnerability evaluation of axially loaded steel built-up laced members II: evaluations.”Earthquake Engineering and Engineering Vibration 7.2, pp. 125-136.

Lehman, D. E., Roeder, C. W., Herman, D., Johnson, S., & Kotulka, B. (2008). “Improved seismic performance of gusset plate connections”. *Journal of Structural Engineering*, 134(6), pp. 890-901.

Lumpkin, E. J., Hsiao, P. C., Roeder, C. W., Lehman, D. E., Tsai, C. Y., Wu, A. C., ... & Tsai, K. C. (2012). “Investigation of the Seismic Response of Three-Story Special Concentrically Braced Frames.” *Journal of Constructional Steel Research*, 77, pp. 131-144.

Roeder, C. W., Lumpkin, E. J., & Lehman, D. E. (2011). “A Balanced Design Procedure for Special Concentrically Braced Frame Connections.” *Journal of Constructional Steel Research*, 67(11), pp. 1760-1772.

Simulia, ABAQUS Finite Element Analysis, www.simulia. com, 2011

Stoakes, C. D., &Fahnestock, L. A. (2010). “Cyclic Flexural Testing of Concentrically Braced Frame Beam-Column Connections”. *Journal of Structural Engineering*, 137(7), pp. 739-747.

Tremblay, R. (2002). “Inelastic Seismic Response of Steel Bracing Members.” *Journal of Constructional Steel Research*, 58(5), pp. 665-701.

Uriz, P. (2005). “Towards earthquake resistant design of concentrically braced steel structures.” University of California, Berkeley.

Yoo, J. H., Roeder, C. W., & Lehman, D. E. (2008). “Analytical Performance Simulation of Special Concentrically Braced Frames.” *Journal of structural engineering*, 134(6), pp. 881-889.